ACKNOWLEDGEMENTS

This study was supported by a grant from the Ministry of Education, Culture, Sports, Science and Technology (No. 20590782), and in part by a Research on Hepatitis, Health and Labor Sciences Research Grants from the Ministry of Health, Labor and Welfare, Japan.

REFERENCES

1. Quaglia A, Tibballs J, Grasso A, et al. Focal nodular hyperplasia-like areas in cirrhosis. *Histopathology* 42:14-21, 2003.
2. Nakashima O, Kurogi M, Yamaguchi R, et al. Unique hypervascular nodules in alcoholic liver cirrhosis: identical to focal nodular hyperplasia-like nodules? *J Hepatol* 41:992-998, 2004.
3. Libbrecht L, Cassiman D, Verslype C, et al. Clinicopathological features of focal nodular hyperplasia-like nodules in 130 cirrhotic explant livers. *Am J Gastroenterol* 101:2341-2346, 2006.
4. Ishak KG, Goodman ZD, Stocker JT. Tumor of the liver and intrahepatic bile ducts. in: Atlas of Tumor Pathology, 3rd ser. Craig JR, Peters RL, Edmondson HA, Eds. Armed Forces Institute of Pathology, Washington DC, 2001:38
5. Huppertz A, Haraida S, Kraus A, et al. Enhancement of focal liver lesions at gadoxetic acid-enhanced MR imaging: correlation with histopathologic findings and spiral CT--initial observations. *Radiology* 234:468-478, 2005.
6. Saito K, Kotake F, Ito N, et al. Gd-EOB-DTPA enhanced MRI for hepatocellular carcinoma: quantitative evaluation of tumor enhancement in hepatobiliary phase. *Magn Reson Med Sci* 4:1-9, 2005.
7. Kim SH, Kim SH, Lee J, et al. Gadoxetic acid-enhanced MRI versus triple-phase MDCT for the preoperative detection of hepatocellular carcinoma. *AJR Am J Roentgenol* 192:1675-1681, 2009.
8. Ichikawa T. MRI in the evaluation of hepatocellular nodules: role of pulse sequences and contrast agents. *Intervirology* 47:252-270, 2004.
9. Kanematsu M, Kondo H, Goshima S, Tsuge Y, Watanabe H. Magnetic resonance imaging of hepatocellular carcinoma. *Oncology* 75 Suppl 1:65-71, 2008.
10. Wanless IR, Mawdsley C, Adams R. On the pathogenesis of focal nodular hyperplasia of the liver. *Hepatology* 5:1194-1200, 1985.
11. Kondo F. Benign nodular hepatocellular lesions caused by abnormal hepatic circulation: etiological analysis and introduction of a new concept. *J Gastroenterol Hepatol* 16:1319-1328, 2001.
12. Kondo F. Focal nodular hyperplasia-like lesions in heavy drinkers. *Intern Med*

48:1117-1123, 2009.

13. Kogita S, Imai Y, Okada M, et al. Gd-EOB-DTPA-enhanced magnetic resonance images of hepatocellular carcinoma: correlation with histological grading and portal blood flow. *Eur Radiol* 20: 2405-2413, 2010.
14. Zech CJ, Grazioli L, Breuer J, Reiser MF, Schoenberg SO. Diagnostic performance and description of morphological features of focal nodular hyperplasia in Gd-EOB-DTPA-enhanced liver magnetic resonance imaging: results of a multicenter trial. *Invest Radiol* 43:504-511, 2008.
15. Narita M, Hatano E, Arizono S, et al. Expression of OATP1B3 determines uptake of Gd-EOB-DTPA in hepatocellular carcinoma. *J Gastroenterol* 44:793-798, 2009.
16. Ohtomo K, Itai Y, Ohtomo Y, Shiga J, Lio M. Regenerating nodules of liver cirrhosis: MR imaging with pathologic correlation. *AJR Am J Roentgenol* 154:505-507, 1990.
17. Kobayashi S, Matsui O, Kamura T, et al. Imaging of benign hypervascular hepatocellular nodules in alcoholic liver cirrhosis: differentiation from hypervascular hepatocellular carcinoma. *J Comput Assist Tomogr* 31:557-563, 2007.
18. Taouli B, Vilgrain V, Dumont E, Daire JL, Fan B, Menu Y. Evaluation of liver diffusion isotropy and characterization of focal hepatic lesions with two single-shot echo-planar MR imaging sequences: prospective study in 66 patients. *Radiology* 226:71-78, 2003.
19. Kim SR, Imoto S, Ikawa H, et al. Focal nodular hyperplasia-like lesion with venous washout in alcoholic liver cirrhosis. *Intern Med* 47:1899-1903, 2008.
20. Sakamoto M, Hirohashi S, Shimosato Y. Early stages of multistep hepatocarcinogenesis: adenomatous hyperplasia and early hepatocellular carcinoma. Hum Pathol 22:172-178, 1991.

FIGURE LEGENDS

Figure 1. Images of the FNH-like nodule in segment 3 in Gd-EOB-DTPA-enhanced MRI

Arrows indicate a 9 mm FNH-like nodule. (A) Low signal intensity before contrast injection, (B) High signal intensity during the hepatic arterial phase, (C) Washout pattern during the equilibrium phase, (D) Low signal intensity during the hepatobiliary phase.

Figure 2. Images of the FNH-like nodule in segment 3 in Gd-EOB-DTPA-enhanced MRI

Arrows indicate the 9 mm FNH-like nodule. (A) No detection of nodule in diffusion-weighted MRI, (B) Low signal intensity on in-phase T1-weighted MRI, (C) Isosignal intensity on opposed-phase T1-weighted MRI, (D) Slightly low signal intensity in T2-weighted MRI, (E) Slightly low signal intensity in SPIO-enhanced MRI.

Figure 3. Surgically resected specimen and histology of the FNH-like nodule

(A) Arrows indicate the FNH-like nodule (15 mm). The nodule is not encapsulated and its margin is difficult to distinguish from the surrounding tissue. (B) The surrounding tissue shows liver cirrhosis (Masson trichrome ×40). (C) Fibrovascular septa with mild lymphocyte infiltrate within the FNH-like nodule (H&E ×100), (D) Unpaired small arteries (arrows) and reactive bile ductules radiating into the parenchyma (arrowheads) within a fibrovascular septum in the FNH-like nodule (H&E ×400).

Figure 4. Cell density, iron deposits and sinusoidal capillarization in the FNH-like nodule and the surrounding tissue. The FNH-like nodule shows increased cell density (A, H&E ×400), remarkable iron deposits in the hepatocyte and/or Kupffer cells (B, Berlin blue ×400) and marked sinusoidal capillarization (C, immunohistochemical staining using anti-CD34 ×400), compared to the surrounding tissue.

Figure 5. Expression of OATP1B3 in surgically resected specimen

Arrows indicate the FNH-like nodule (A). The expression of OATP1B3 is nearly absent in the nodule (B, ×400), but is diffusely found in the surrounding tissue (C, ×400). OATP1B3 was immunohistochemically detected using anti-OATP1B3.

Figure 1

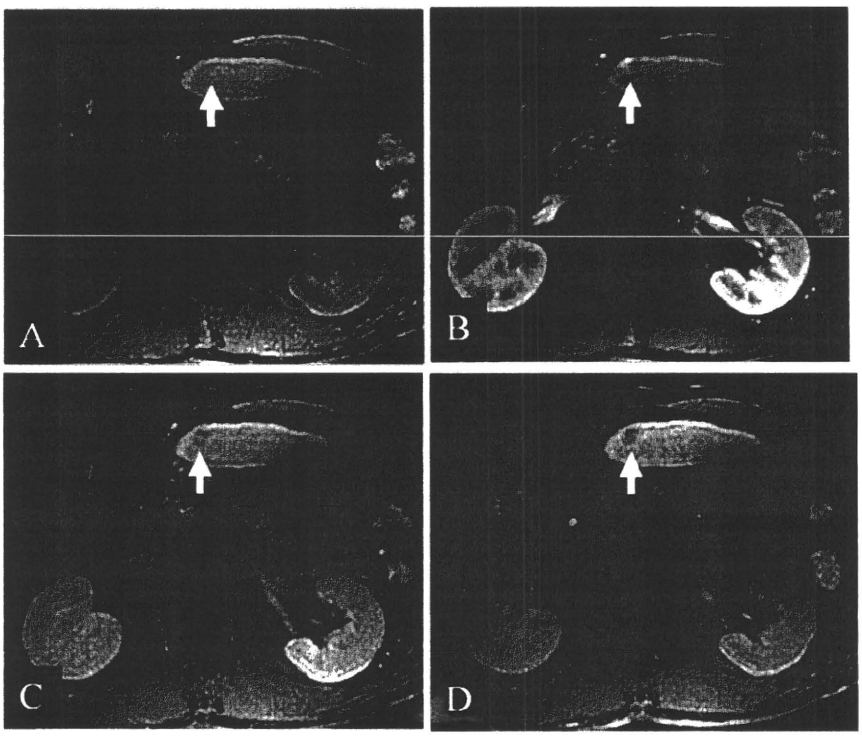

Figure 2

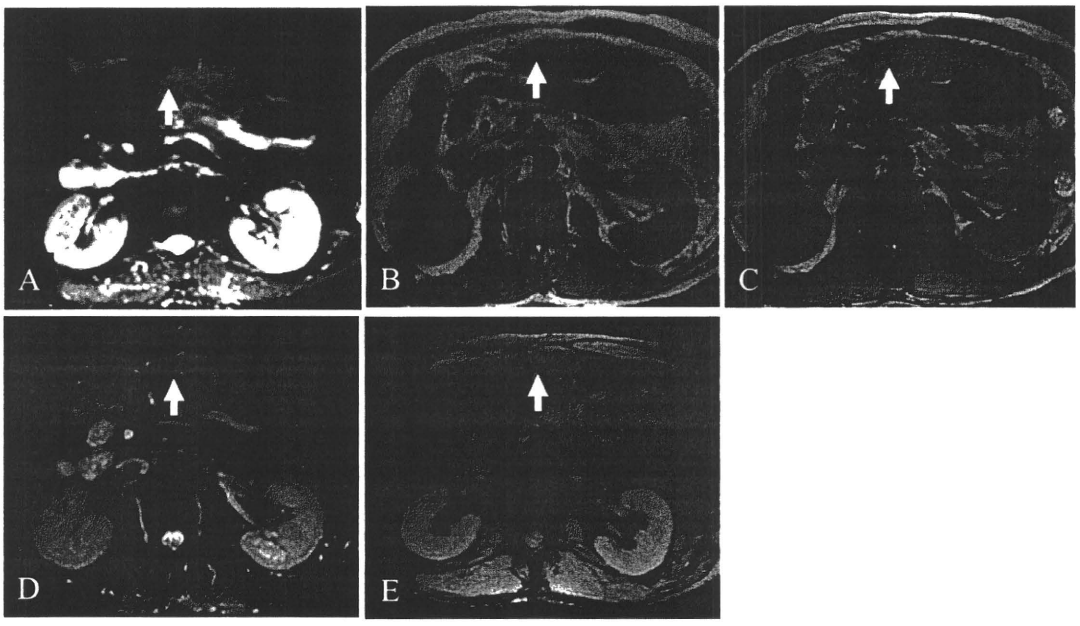

Figure 3

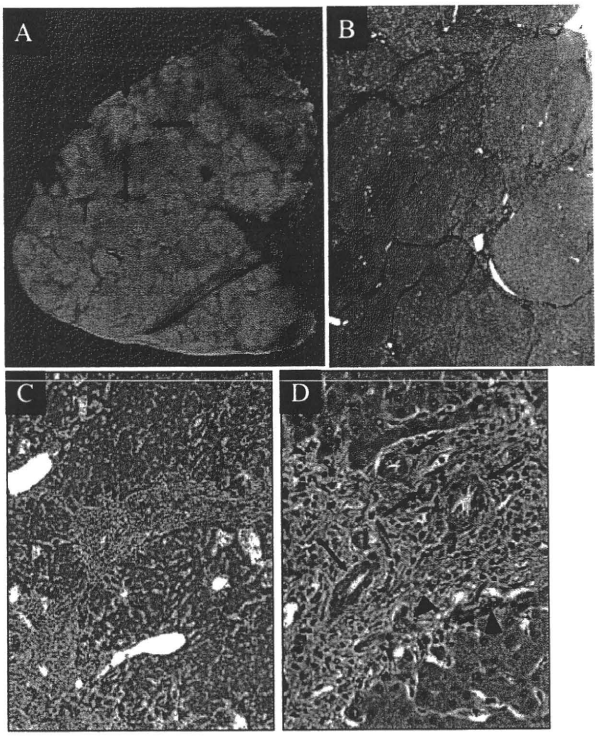

Figure 4

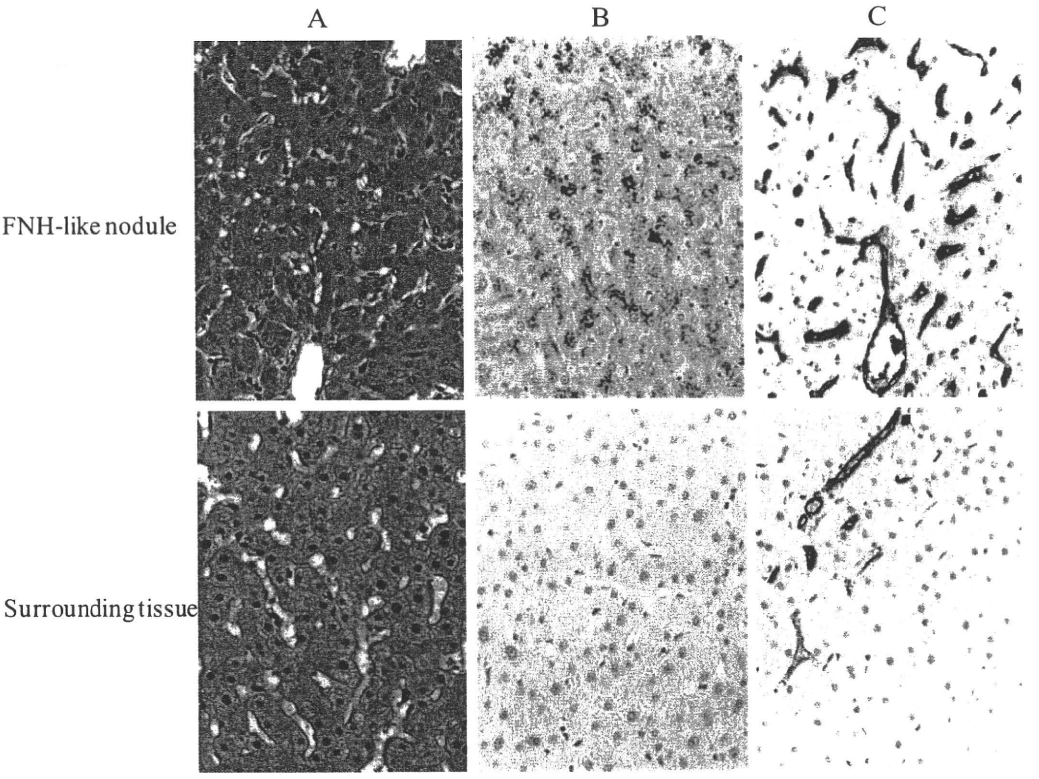

Figure 5

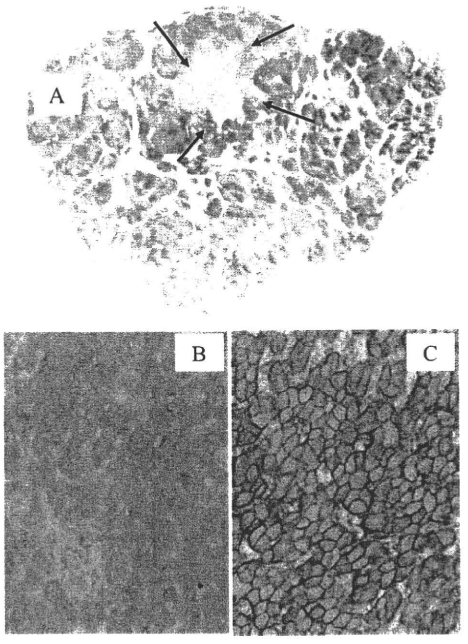

The rs8099917 Polymorphism, Determined by a Suitable Genotyping Method, is a Better Predictor for Response to Pegylated Interferon- α /Ribavirin Therapy in Japanese Patients than Other SNPs Associated with IL28B

Running Title: Best Predictor for Treatment of CHC Patients

Kiyoaki Ito [1*], Katsuya Higami [1*], Naohiko Masaki [1], Masaya Sugiyama [1], Motokazu Mukaide [1], Hiroaki Saito [1], Yoshihiko Aoki [1], Yo Sato [1], Masatoshi Imamura [1], Kazumoto Murata [1], Hideyuki Nomura [2], Shuhei Hige [3], Hiroshi Adachi [4], Keisuke Hino [5], Hiroshi Yatsuhashi [6], Etsuro Orito [7], Satomi Kani [8], Yasuhito Tanaka [8], Masashi Mizokami [1]

[1] The Research Center for Hepatitis and Immunology, National Center for Global Health and Medicine, Ichikawa, [2] The Center for Liver Diseases, Shin-Kokura Hospital, Kitakyushu, [3] Department of Internal Medicine, Hokkaido University Graduate School of Medicine, Sapporo, Department of Virology and Liver Unit, [4] Tonami General Hospital, Tonami, [5] Division of Gastroenterology, Department of Medicine, Kawasaki Medical School, Okayama, [6] Clinical Research Center, NHO Nagasaki Medical Center, Nagasaki, [7] Department of Gastroenterology and Hepatology, Nagoya Daini Red Cross Hospital, [8] Nagoya City University Graduate School of Medical Sciences, Nagoya, Japan

*These authors contributed equally to the manuscript

Corresponding author: Masashi Mizokami, M.D., Ph.D.,
The Research Center for Hepatitis and Immunology, National Center for Global Health and Medicine.
Address: 1-7-1, Konodai, Ichikawa 272-8516, Japan.
Tel.: +81-(0)47-372-3501
Fax: +81-(0)47-375-4766
E-mail: mmizokami@hospk.ncgm.go.jp.

ABSTRACT

We focused on determining the most accurate and convenient genotyping methods and most appropriate SNP among four such polymorphisms associated with IL28B in order to design tailor-made therapy for chronic hepatitis C patients. Firstly, five different methods (direct sequencing, high-resolution melting analysis (HRM), Hybridization probe (HP), InvaderPlus assay (Invader), and TaqMan SNP genotyping assay (TaqMan)) were developed for genotyping four SNPs (rs11881222, rs8103142, rs8099917 and rs12979860) associated with IL28B and their accuracy was compared in 292 Japanese patients. Next, the four SNPs associated with IL28B were genotyped by Invader in 416 additional Japanese patients and the response to PEG-IFN/RBV treatment was evaluated when the four SNPs were not in linkage disequilibrium (LD). HRM failed to genotype one of the four SNPs in five patients. In two of 287 patients, the results of genotyping rs8099917 by direct sequencing differed from the results of the other three methods. The methods of HP, TaqMan and Invader were accurate for determining the SNPs associated with IL28B. In ten of the 708 (1.4%) patients, the four SNPs were not in LD. Eight of nine (88.9%) patients whose rs8099917 was homozygous for the major allele were virological responders, even though one or more of the other SNPs were heterozygous. The methods of HP, TaqMan and Invader were suitable to determine the SNPs associated with IL28B. The rs8099917 polymorphism should be the best predictor for the response to the PEG-IFN/RBV treatment among Japanese chronic hepatitis C patients.

Key Words: IL28B, SNP, chronic hepatitis C, tailor-made treatment, PEG-IFN/RBV

INTRODUCTION

Hepatitis C virus (HCV) infection is a global health problem, with worldwide estimates of 120-130 million carriers (1). Chronic HCV infection can lead to progressive liver disease, resulting in cirrhosis and complications including decompensated liver disease and hepatocellular carcinoma (25). The current standard-of-care treatment for suitable patients with chronic HCV infection consists of pegylated interferon alpha 2a or 2b (PEG-IFN) given by injection in combination with oral ribavirin (RBV), for 24 or 48 weeks, dependent on HCV genotype. Large-scale treatment programs in the United States and Europe showed that 42-52% of patients with HCV genotype 1 achieved a sustained virological response (SVR) (4, 8, 13), and similar results were found in Japan. This treatment is associated with well-described side effects (such as a flu-like syndrome, hematologic abnormalities and neuropsychiatric events) resulting in reduced compliance and fewer patients completing treatment (3). It is valuable to predict an individual's response before treatment with PEG-IFN/RBV to avoid these side-effects, as well as to reduce the treatment cost. HCV genotype, in particular, is used to predict the response: patients with HCV genotype 2 or 3 have a relatively high rate of SVR (70-80%) with 24 weeks of treatment, whereas those infected with genotype 1 have a much lower rate of SVR despite 48 weeks of treatment (8).

Recently, we reported from genome-wide association studies (GWAS) that several highly correlated common single nucleotide polymorphisms (SNPs), located in the vicinity of the IFN-lambda 3 (IL28B) gene on chromosome 19, are implicated in NVR (non-virological response) to PEG-IFN/RBV among patients with HCV genotype 1 (21).

At almost exactly the same time as our report, the association between response to PEG-IFN/RBV and SNPs associated with IL28B was reported from the results of GWAS by two other groups (7, 19). Determining these SNPs associated with IL28B before PEG-IFN/RBV treatment will provide extremely valuable information, because the patients predicted as NVR to PEG-IFN/RBV treatment could avoid the treatment. There are two questions to be asked before using these SNPs in clinical practice: which methods for genotyping these SNPs are efficient and which SNP is most informative in cases where the SNPs are not in linkage disequilibrium (LD). We have developed five different methods for detecting the SNPs associated with IL28B and compared their accuracy to establish the most efficient genotyping method. The response to PEG-IFN/RBV treatment was evaluated, when the SNPs associated with IL28B were not in LD, to determine the best SNP to predict the response to PEG-IFN/RBV treatment.

MATERIALS AND METHODS

Study population

Samples were obtained from 708 Japanese chronic hepatitis C patients and divided into groups of 292 (145 males, 147 females; mean age: 57.2 years) and 416 patients (194 males, 222 females; mean age: 56.6 years) for the first and second stages (Table 1). In the first stage, we focused on analyzing the effective methods for determining the genotypes of four SNPs (rs11881222, rs8103142, rs12979860, and rs8099917) associated with IL28B (Figure 1A). Figure 2 shows the location of these four SNPs in chromosome 19; rs11881222 and rs8103142 are located in the IL28B gene and

rs12979860 and rs8099917 are located downstream from IL28B. The results of genotyping the four SNPs by five different methods, described below, were compared and evaluated for consistency. For this first stage, the 292 chronic hepatitis C patients were recruited from the National Center for Global Health and Medicine, Hokkaido University Hospital, Tonami General Hospital, and Shin-Kokura Hospital in Japan (Table 1). From the results of the first stage, the InvaderPlus assay was chosen as one of the best methods to determine the genotypes of the four SNPs associated IL28B and was used for genotyping 416 patients (Figure 1B), recruited from NHO Nagasaki Medical Center, Nagoya City University Hospital, Nagoya Daini Red Cross Hospital, and Kawasaki Medical University Hospital in Japan, in the second stage (Table 1). We then focused on ten patients whose four SNPs were found in the first and second stages not to be in LD and investigated the response to PEG-IFN/RBV treatment in detail in these patients. Informed consent was obtained from each patient who participated in the study. This study was conducted in accordance with provisions of the Declaration of Helsinki.

Definition of treatment responses

Non-virological response (NVR) was defined as less than a 2-log-unit decline in the serum level of HCV RNA from the pre-treatment baseline value, within the first 12 weeks, or detectable viremia 24 weeks after treatment. Virological response (VR) was defined in this study as the achievement of sustained VR (SVR) or transient VR (TVR); SVR was defined as undetectable HCV RNA in serum 6 months after the end of treatment, whereas TVR was defined as a reappearance of HCV RNA in serum after

treatment was discontinued in a patient who had undetectable HCV RNA during the therapy or achieved more than 2-log-unit decline within the first 12 weeks after treatment.

DNA extraction

Whole blood was collected from all participants and centrifuged to separate buffy coat. Genomic DNA was extracted from the buffy coat with GENOMIX (Talent SRL, Italy).

Five different genotyping methods

Four SNPs (rs11881222, rs8103142, rs12979860 and rs8099917; shown in Figure 2) were determined in 292 patients by five different genotyping methods. We developed the five methods (direct sequencing, high-resolution melting analysis (HRM), Hybridization probe (HP), InvaderPlus® assay (Invader), and TaqMan SNP genotyping assay (TaqMan) to determine the genotypes of the rs11881222 and rs8103142 polymorphisms. We also developed four different methods (direct sequencing, HRM, HP and Invader) to determine the genotypes of the rs12979860 and rs8099917 polymorphism. The genotype of rs12979860 was also determined by the TaqMan genotyping method developed by Duke University and the genotype of rs8099917 was also determined by TaqMan® Pre-Designed SNP Genotyping Assay. Figure 3, 4 and 5 show the primers and probes for each genotyping method. Because the sequence of IL28B is very similar to those of IL28A, Il29 and a homologous sequence upstream of IL28B, we had to design the primers and probe for each method to distinguish IL28B

from the others sequencies. Firstly, primers were designed using Visual OMP Nucleic Acid software. Then, we confirmed that the candidate primers should not amplify sequences other than the target region using UCSC Genome Browser. Next, we confirmed that the amplicon was resolved as a single band, when the PCR products amplified by the primers under evaluation were electrophoresed. Finally, we had to optimize each set of primers and probe for each method (Figure 3-5 and Supplementary table).

Direct Sequencing

PCR was carried out using 12.5 μl AmpliTaq Gold 360 Master Mix (Applied Biosystems), 10 pmol of each primer and 10ng of genomic DNA under the following thermal cycler conditions: stage 1, 94°C for 5 min; stage 2, 94°C for 30 s, 65°C for 30 s, 72°C for 45 s, for a total of 35 cycles; stage 3, 72°C for 7 min. For sequencing, 1.0 μl of the PCR products were incubated with the use of a BigDye Terminator v3.1 Cycle Sequencing Kit (Applied Biosystems). After ethanol purification, the reaction products were applied to the Applied Biosystems 3130xl DNA Analyzer.

HRM analysis

HRM analysis was performed on a LightCycler 480 (LC480; Roche Diagnostics) as described previously (6, 15, 24). We designed pairs of primers flanking each SNP (Figure 3-5) to amplify DNA fragments shorter than 200 bp. PCR was performed in a 20 μl volume containing: 10 μl LightCycler 480 High-Resolution Melting Master mix

(Roche Applied Science), 4 pmol of each primer and 10 ng genomic DNA. The cycling conditions were as follows: SYBR Green I detection format; 1 cycle of 95°C for 10 min, 50 cycles of 95°C for 5 s, 60°C for 10s, and 72°C for 20 s; followed by an HRM step of 95°C for 1 min, 40°C for 1 min, 74°C for 5 s, and continuous acquisition to 90°C at 25 acquisitions per 1°C. HRM data were analyzed using the Gene Scanning Software (Roche Diagnostics).

Hybridization probe

We designed oligonucleotide primers and hybridization probes for the four SNPs (Figure 3-5). All assays were performed using the LC480 as described previously (5, 18). The amplification mixture consisted of 4 μl of 5 *X* reaction mix (LightCycler 480 genotyping master, Roche Diagnostics), 5 pmol of each oligonucleotide primer, 3.2 pmol of each oligonucleotide probe, and 10ng of template DNA in a final volume of 20 μl. Samples were amplified as follows: 45 cycles of denaturation at 95°C for 10 s, annealing at 60°C for 10 s, and an extension at 72°C for 20 s. The generation of target amplicons for each sample was monitored between the annealing and the elongation steps at 610 and 640 nm. Samples positive for target genes were identified by the instrument at the cycle number where the fluorescence attributable to the target sequences exceeded that measured for background. Those scored as positive by the instrument were confirmed by visual inspection of the graphical plot (cycle number versus fluorescence value) generated by the instrument.

InvaderPlus assay

The InvaderPlus® assay, which combines PCR and the Invader reaction (11, 12) was performed using the LC480. The enzymes used in Invader Plus are native *Taq* polymerase (Promega Corporation,Madison, WI) and Cleavase enzyme (Third Wave Technologies,Madison, WI). The reaction is configured to use PCR primers with a melting temperature (*Tm*) of 72°C and Invader detection probe with a target-specific *Tm* of 63°C. The invader oligonucleotide overlaps the probe by one nucleotide, forming at 63°C overlap flap substrate for the Cleavase enzyme. The first step of Invader Plus is PCR target amplification, in which the reaction is subjected to 18 cycles of a denaturation step (95°C for 15s) and hybridization and extension steps (70°C for 1min). At the end of PCR cycling, the reaction mixture is incubated at 99°C for 10 min to inactivate the *Taq* polymerase. Next, the reaction temperature is lowered to 63°C for 15 to 30 min to permit the hybridization of the probe oligonucleotide and the formation of the overlap flap structure. Data were analyzed by endpoint genotyping software (Roche diagnostics).

TaqMan assay

The rs8099917 polymorphism was determined using TaqMan® Pre-Designed SNP Genotyping Assays, as recommended by the manufacturer. The TaqMan assay for determining the genotype of rs12979860 was kindly provided by Dr David B. Goldstein at Duke University. We designed primers and probes for TaqMan genotyping assays for the other two SNPs. Each genomic DNA sample (20 ng) was amplified using TaqMan

Universal PCR master mix reagent (Applied Biosystems, Foster City, CA) combined with the specific TaqMan SNP genotyping assay mix, corresponding to the SNP to be genotyped. The assays were carried out using the LC 480 (Roche Applied Science) and the following conditions: 2 min at 50°C, 10 min at 95°C, 40 cycles: 15 sec at 95°C, and 1 min at 60°C. Data were analyzed by endpoint genotyping software (Roche diagnostics).

RESULTS

Genotyping for four SNPs associated with IL28B was failed by HRM in five cases

Figure 1A shows the patient's flow chart of the first stage. Genotyping of four SNPs (rs11881222, rs8103142, rs12979860 and rs8099917) was attempted by five different methods (direct sequencing, HRM, HP, Invader and TaqMan) in 292 patients. In five cases, one of the four SNPs could not be genotyped by HRM. Therefore, we excluded the HRM method from further study. Genotyping failures by HRM were two cases for rs11881222, two cases for rs8103142 and one case for rs8099917.

Consistencies of four different methods to determine genotypes for four SNPs associated with IL28B.

Consistencies among the results of genotyping by the remaining four methods were 100%, except for the results of rs8099917 (Table 2). For rs8099917, the results determined by direct sequencing were inconsistent with the other three methods in two cases (Table 2 and 3). HP, TaqMan, and Invader methods were accurate and reliable for genotyping the four SNPs associated with IL28B. Invader was chosen for genotyping in

the second stage, because the analysis time was the shortest and the sensitivity was the greatest of the three methods (HP, TaqMan and Invader) as reported previously (20).

Genotyping Error for rs8099917 by direct sequence due by novel SNP

In two cases, the results of genotyping for rs8099917 by direct sequencing were inconsistent with the results by the other methods (Table 3). Direct sequencing determined the genotype for rs8099917 as T/T in cases 1 and 2, however, the other three genotyping methods (HP, Invader, and TaqMan) determined the genotypes for rs8099917 as T/G in both cases. Further study using alternative primers for direct sequencing revealed that the correct genotypes were T/G and revealed a novel minor SNP present in at the forward primer binding site in these two cases (data on file) and which interfered with the PCR amplification step (Figure 3).

Distribution of haplotypes among four SNPs associated with IL28B.

In the first stage, the four SNPs were in LD in 281 (98.6%) of 285 cases and not in LD in the remaining four (1.4%). The first stage revealed five different haplotypes (haplotype 1-5; Table 4). In haplotypes 1-3, the four SNPs were in LD (haplotype 1: homozygous of major allele among 4 SNPs; n=198 [69.5%], haplotype 2: heterozygous among 4 SNPs; n=79 [27.7%], and haplotype 3: homozygous of minor allele among 4 SNPs; n=4 [1.4%]). In haplotype 4 (3 cases) rs11881222, rs8103142, rs12979860 and rs8099917 were AG, TC, CT, and TT, respectively. In haplotype 5 (one case) rs11881222, rs8103142, rs12979860 and rs8099917 were AA, TT, CT, and TT,